

Mass Transfer of Polynuclear Aromatic Hydrocarbons from Complex DNAPL Mixtures

SUPARNA MUKHERJI,[†]
CATHERINE A. PETERS,[‡] AND
WALTER J. WEBER, JR.*[†]

*Environmental and Water Resources Engineering,
Department of Civil and Environmental Engineering,
The University of Michigan, Ann Arbor, Michigan 48109-2125,
and Department of Civil Engineering and Operations
Research, Princeton University, Princeton, New Jersey 08544*

Parameters governing the rates of mass transfer of the individual components of four synthetic dense non-aqueous phase liquid (DNAPL) mixtures into the aqueous phase were evaluated. The DNAPL mixtures, composed of toluene and eight polynuclear aromatic hydrocarbons (PAHs), were designed to serve as models for coal tars and creosotes. The reactor employed provided a relatively stable interface between internally mixed but segregated aqueous and DNAPL phases. Two parameters, the aqueous phase concentration at equilibrium and the overall film mass transfer coefficient, were quantified by simulating aqueous concentration profiles with a mass-transfer-limited rate model using a statistical parameter search and data fitting routine. DNAPL phase activity coefficient values for the various compounds derived from equilibrium aqueous phase concentrations were typically within a factor of 2 of Raoult's law prediction of unity; refinement of fugacity ratio estimates for the solid PAHs brought the values even closer to unity. Film transfer coefficients for all components of the mixtures studied were similar in magnitude, in the range $0.8-3 \times 10^{-3}$ cm/s. No significant variations of the film transfer coefficient for naphthalene were noted across the DNAPL mixtures, over which the mole fraction of this compound was varied from 0.05 to 0.25.

Introduction

Polynuclear aromatic hydrocarbons (PAHs) are often present in the environment as components of such dense non-aqueous phase liquids (DNAPLs) as coal tars and creosotes. Such environmental DNAPLs are usually complex and incompletely characterized mixtures and often contain components that may pose significant health hazards because of their toxicity and/or carcinogenicity (1). The dissolution of individual PAHs from such DNAPLs into raw water sources has on many occasions led to aqueous concentrations exceeding safe drinking water standards (1, 2). Many PAHs are only sparingly soluble, and large volumes of water can therefore be contaminated by small amounts of DNAPL. Efforts directed at isolation and removal of DNAPL sources are often constrained by difficulties in identifying their locations (3), thus requiring resort to water-based remediation technologies, i.e., *in-situ* or *ex-situ* water treatment schemes.

* To whom correspondences should be addressed. E-mail: wjwjr@engin.umich.edu; phone: (313) 763-1464; fax: (313)-763-2275.

[†] The University of Michigan.

[‡] Princeton University.

The low aqueous phase concentrations generally associated with the slow mass transfer of constituents from DNAPL phases frequently render such schemes ineffective (4, 5). DNAPL component mass transfer rates to aqueous phases thus have 2-fold significance, affecting as they do both the environmental impact of DNAPL contamination and the likely success of water-based remediation technologies.

Mass fluxes from DNAPL phases to water resulting from rate-limited interphase mass transfer processes are commonly considered to be proportional to a linear concentration difference driving force, i.e., to the difference between the expected aqueous phase equilibrium concentration and the actual bulk aqueous phase concentration (6). The constant of proportionality, referred to as the film mass transfer coefficient, is inversely related to the overall mass transfer resistance comprised by the boundary layers on each side of the interface separating the bulk phases, although for hydrophobic compounds such as PAHs the aqueous side boundary layer resistance is typically considered to be rate-limiting (5, 7). This film transfer coefficient is system specific in nature and depends upon the relative velocities and level of microturbulence in the vicinity of the interface. However, as the impact of turbulence at the interface is minimized, it is expected to approach a limiting intrinsic value that is a function of the diffusivity of a given solute in each of the two liquid phases.

The equilibrium concentration of a non-aqueous phase constituent in the aqueous phase can be determined on the basis of multicomponent liquid-liquid equilibrium theory, which predicts the equality of fugacities of a species between phases at equilibrium. Moreover, with the assumption that the aqueous phase activity coefficient of a component is unaffected by the dissolution of the other species comprising the non-aqueous phase liquid (8), the following equation can be derived:

$$C_{e,i}^a = \frac{X_i^n \alpha_i^n C_{s,i}}{(f_i^s / f_i^l)} \quad (1)$$

where the subscript *i* denotes quantities pertaining to component *i*, the superscripts *a* and *n* denote quantities pertaining respectively, to the aqueous and non-aqueous phases, C_s is the pure compound solubility, C_e is the equilibrium concentration, α is the activity coefficient, X is the mole fraction, and f^s and f^l are the fugacities in the pure solid and pure liquid states, respectively. The ratio of the solid to liquid state fugacities is referred as the fugacity ratio, and the ratio of the pure compound solubility to the fugacity ratio is the subcooled liquid solubility. For non-aqueous phase liquids comprised of structurally similar components, the Raoult's law characterization of ideal behavior of chemical species in the NAPL phase (i.e., NAPL phase activity coefficients of unity), is another common assumption. This assumption implies that each compound behaves in the NAPL phase as if it existed in its own pure liquid phase. Interactions between different constituent molecules and differences in the sizes and shapes of various species comprising a NAPL mixture can, however, cause deviations from ideal behavior.

The general conformity of the partitioning behavior of PAH components between aqueous and non-aqueous phases with Raoult's law predictions have been demonstrated in several studies involving coal tars and coal tar-contaminated soils (9-12). Most of these studies employed batch equilibration techniques and demonstrated strong correlations between NAPL-water partition coefficients and subcooled liquid solubilities. Deviations exceeding a factor of 2 have been noted in a few instances however (10, 13, 14). It is difficult in studies with field samples to rigorously test the

TABLE 1. Properties of DNAPL Mixture Components

component	mol wt (g/mol)	melting point (°C)	solid/liquid fugacity ratio	aqueous solubility (mg/L)	aqueous diffusivity (cm ² /s × 10 ⁶)
toluene	92.13	-95	1.000	530	9.10
naphthalene	128.19	81	0.283	31	7.99
1-methylnaphthalene	142.20	-22	1.000	28	7.36
2-ethylnaphthalene	156.23	-7.4 ^a	1.000	8	6.84
acenaphthene	154.21	96	0.198	3.80	7.27
fluorene	166.20	116	0.126	1.90	6.93
phenanthrene	178.20	101	0.177	1.10	6.70
fluoranthene	202.30	111	0.141	0.26	6.36
pyrene	202.30	156	0.051	0.13	6.42

^a Based on experiments in our laboratories, this value is thought to be more accurate than the value of -70 °C reported in Mackay et al. (23).

validity of Raoult's law due to uncertainties associated with the estimation of such bulk phase properties as molecular weights and densities. Moreover, the low mole fractions of the compounds of interest in complex NAPLs often result in aqueous phase compositions close to analytical detection limits, thereby increasing errors inherent to measured values.

Liquid-liquid mass transfer in packed columns, in slurry systems, and in dispersed liquid-liquid systems is typically described in terms of a lumped mass transfer coefficient, which is given in turn by the product of the film transfer coefficient and the specific interfacial area. Information deficiencies with respect to the specific interfacial areas involved in such reactor systems prevents a direct determination of the film transfer coefficient, although values can be estimated using system-specific correlations (4, 5, 15, 16). In contrast, mass transfer in non-dispersed liquid-liquid systems having easily quantifiable specific interfacial areas can be described more directly in terms of film mass transfer coefficients. Ghoshal et al. (17) determined film transfer coefficient values of 3.05×10^{-4} and 2.44×10^{-4} cm/s for the aqueous dissolution of naphthalene from a single droplet of two different coal tars in gently mixed systems. Several studies have reported PAH mass transfer rates from films of LNAPLs (NAPLs lighter than water) floating above an adequately mixed aqueous phase. By way of several examples, Ghoshal et al. (17) reported the film transfer coefficient of naphthalene from heptamethylnonane as 1.67×10^{-3} cm/s, Efrogmson and Alexander (18) reported that of phenanthrene from various aliphatic NAPLs as 5×10^{-4} – 3×10^{-3} cm/s, Southworth et al. (7) reported for toluene, naphthalene, and 1-methylnaphthalene from heptane as approximately 5×10^{-4} cm/s, and Herbes et al. (19) also reported for aromatic components from coal liquefaction oils (LNAPL mixtures) as 5×10^{-4} cm/s. Luthy et al. (9) demonstrated the formation of interfacial films on coal tar-water interfaces and their impacts on lowering overall mass transfer rates. These films are thought to be the result of bonding between water molecules and coal tar constituents (20).

The focus of the research described here was the quantification of two parameters expected to govern rates of mass transfer of each component from multicomponent DNAPL mixtures into water; specifically, the mass transfer coefficient and the aqueous phase equilibrium concentration, the latter of which translates to a DNAPL phase activity coefficient. Our broader goals were to determine how interfacial mass transfer parameters vary among the individual PAH components of specific DNAPL mixtures and how these parameters vary for each component with systematic variations in DNAPL composition. Compositionally well-defined synthetic mixtures were used to avoid the uncertainties and variabilities typically associated with environmental DNAPLs. The rate experiments were conducted in a non-dispersed liquid-liquid system having a relatively quiescent interface separating internally mixed bulk phases. Mass transfer parameters were determined for each of the nine components in four synthetic

mixtures, varying primarily in their respective naphthalene mole fractions. Raoult's law was not used to predict equilibrium aqueous phase concentrations because deviations of the order of a factor of 2 or more were considered unacceptable for estimation of rate parameters. Instead, the DNAPL phase activity coefficient was determined from experimentally measured values of equilibrium aqueous phase concentrations, and the validity of Raoult's law was then tested. Although values of mass transfer coefficients are by nature system specific, values determined with the reactor employed here are believed to approach intrinsic film transfer coefficient values.

Materials and Methods

Toluene and the individual PAH components (obtained in purity $\geq 98\%$ from Aldrich Chemical Co.) of the synthetic DNAPL mixtures are identified, and their properties are listed in Table 1. The aqueous diffusivities were estimated from the Hayduk-Laudie correlation (21); the solubility of toluene obtained from Weber and DiGiano (6), the melting point of 2-ethylnaphthalene obtained from Lide and Frederikse (22), and all other property values obtained from Mackay et al. (23). The fugacity ratio estimates provided in Mackay et al. are based on an assumption of a constant entropy of fusion of $13.5 \text{ cal mol}^{-1} \text{ K}^{-1}$ for all organic compounds and also neglect the impact of specific heats of fusion, which are typically considered negligible.

Preparation of DNAPL Mixtures. The DNAPL mixtures were synthesized with nine aromatic components (primarily PAHs, Table 1) typically present in coal tars and creosotes such that no single component was predominant. Six of the components normally exist as solids in pure form at ambient temperatures, and careful consideration was therefore required in designing the DNAPL mixtures to ensure liquid phase stability. The maximum mole fraction, $(X_i^n)_{\max}$, or solubility of a solid in a pure non-aqueous phase liquid can be obtained from specific thermodynamic considerations (24); i.e.

$$(X_i^n)_{\max} = \frac{1}{\alpha_i^n} (f_i^s/f_i^l) \approx (f_i^s/f_i^l) \quad (2)$$

This equation can be applied to a multicomponent system in which the components form a single non-aqueous liquid phase at all compositions, if it is assumed that each solid phase that exists in equilibrium with the NAPL is a pure solid. Moreover, for a NAPL mixture composed of structurally similar components, the activity coefficients of those components may be assumed to be unity, in which case the ideal solubility of a solid in a multicomponent liquid expressed in terms of its mole fraction is represented by its fugacity ratio. Peters et al. (25) provide a detailed discussion on the stability of multicomponent systems containing PAHs.

The composition of a stock DNAPL mixture devoid of naphthalene and toluene was first designed. For an ideal

TABLE 2. Composition and Bulk Properties of DNAPL Mixtures

components	mol fractions			
	DNAPL-I	DNAPL-II	DNAPL-III	DNAPL-IV
toluene	0.05	0.05	0.04	0.03
naphthalene	0.00	0.05	0.10	0.25
1-methylnaphthalene	0.29	0.28	0.26	0.22
2-ethylnaphthalene	0.14	0.13	0.13	0.11
acenaphthene	0.15	0.14	0.14	0.11
fluorene	0.07	0.07	0.06	0.05
phenanthrene	0.13	0.12	0.12	0.10
fluoranthene	0.12	0.11	0.10	0.09
pyrene	0.05	0.05	0.05	0.04
mixture properties	av property values			
	DNAPL-I	DNAPL-II	DNAPL-III	DNAPL-IV
mol wt (g/mol)	160.2	158.5	157.0	152.2
density (g/mL)	1.065	1.062	1.060	1.055
viscosity $\times 10^2$ (g cm ⁻¹ s ⁻¹)	5.05	4.94	4.65	4.00

DNAPL phase, the sum of mole fractions of liquid components will be minimum for a composition in which all solid components exist at their ideal solubility limit, i.e., such that their mole fraction equals their fugacity ratio at ambient temperature. For the stock DNAPL, this minimum sum of mole fraction of liquid components was determined as 0.31. To incorporate a safety factor for stability to allow for some non-ideality and temperature fluctuations, the sum of mole fractions of the liquid components (1-methylnaphthalene and 2-ethylnaphthalene) were increased to about 0.45, and the mole fractions of all solid components were arbitrarily reduced to levels below their fugacity ratio such that the sum of mole fractions of all components equaled unity. Thus, a composition was designed such that no single compound was predominant, as is typically the case for environmental NAPLs. However, due to the limited number of compounds used, this correspondingly increased the mole fractions above those typically observed in environmental NAPLs comprised by a multitude of compounds.

A stock DNAPL mixture devoid of naphthalene was first prepared by dissolving predetermined amounts of 1-methylnaphthalene, 2-ethylnaphthalene, acenaphthene, fluorene, phenanthrene, fluoranthene, and pyrene in toluene. The relative amount of each component added was determined on the basis of the constraints discussed above. The bulk of the toluene was then removed, first by evaporation in a rotary evaporator (Bucchi Rotovapor Model R-110) and then by purging with nitrogen in a fritted gas washing bottle until the DNAPL level in the bottle stabilized. The residual mole fraction of toluene at this point was less than 0.05. Three other synthetic DNAPL mixtures were then prepared by adding varying amounts of naphthalene to aliquots of the stock, yielding mixtures having naphthalene mole fractions of 0.05, 0.1, and 0.25. The highest mole fraction of naphthalene was chosen to be lower than its ideal solubility. Table 2 summarizes the compositions and properties of the DNAPL mixtures, all of which existed as stable liquids under ambient conditions. The DNAPL phase mole fractions were determined from DNAPL phase concentration measurements. The molecular weights were determined as number-averaged molecular weights. The density and viscosity values were measured in the laboratory using a specific gravity balance and a capillary tube viscometer, respectively.

Mass Transfer Experiments. The reactor depicted schematically in Figure 1 was designed to facilitate the establishment and maintenance of a known and reasonably constant interfacial area of 4.9 cm² between the aqueous and DNAPL phases at an approximately fixed spatial position and to provide complete internal mixing within each phase. Al-

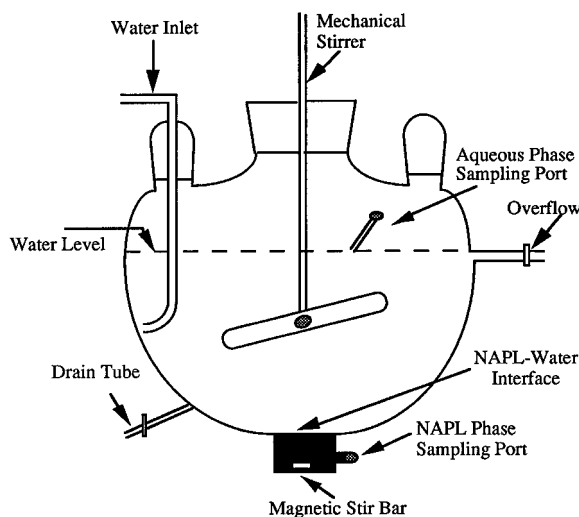


FIGURE 1. Schematic of reactor used for the mass transfer rate studies.

though provisions for aqueous phase flow were made in the reactor design and fabrication, all experiments reported here were conducted in batch mode. The reactor consisted of two volumetric sections, a 1000-mL three-necked flask fused to a cylindrical reservoir at the bottom, with a sampling port in each section and an overflow tube and drain port in the upper section. Water could be admitted through a side neck inlet designed to prevent disturbance of the pre-established water/DNAPL interface. Ground glass joints were employed to minimize volatilization losses.

The aqueous phase was mixed internally by a glass impeller fitted through the central neck and driven by a constant speed subfractional AC gear motor; the DNAPL phase was mixed by a Teflon-clad magnetically driven stirrer. Internal mixing of the aqueous and DNAPL phases was considered necessary to ensure completely mixed conditions in both bulk phases and for samples to be representative of bulk phase conditions. Initial stirring of the aqueous phase at an impeller speed of 60 rpm caused significant disturbance at the interface; a lower value of 39 rpm was found to reduce the disturbance significantly while still providing good internal mixing of the phase. Aqueous phase stirring at lower speeds was not attempted. To ensure the effectiveness of mixing at 39 rpm, a washout study was conducted by sampling the aqueous phase over a duration of about 12 h, after injecting a slug of calcium chloride through the aqueous phase sampling port while operating the reactor in the flow-through mode at a flow rate of 1.95 mL/min. The calcium chloride concentration was determined using atomic absorption spectroscopy. The effectiveness of mixing is illustrated in Figure 2 by the close match between the experimental washout profile and the ideal reactor model prediction given by

$$\frac{C_i^a}{C_{i,0}^a} = \exp\left(\frac{-Qt}{V^a}\right) \quad (3)$$

where V is the volume, Q is the aqueous flow rate, C is the concentration, t is time, and the subscript 'o' denotes the initial condition. The aqueous phase was stirred at 39 rpm for all experiments. The magnetic stirrer setting for mixing the DNAPL phase was selected to result in minimal disturbance at the interface while ensuring complete mixing. The effectiveness of mixing was tested by filling the cylindrical section with 20 mL of liquid and injecting a slug of dye through the DNAPL phase sampling port while mixing the contents magnetically at the desired setting. The dye was uniformly dispersed throughout the entire volume in a few minutes.

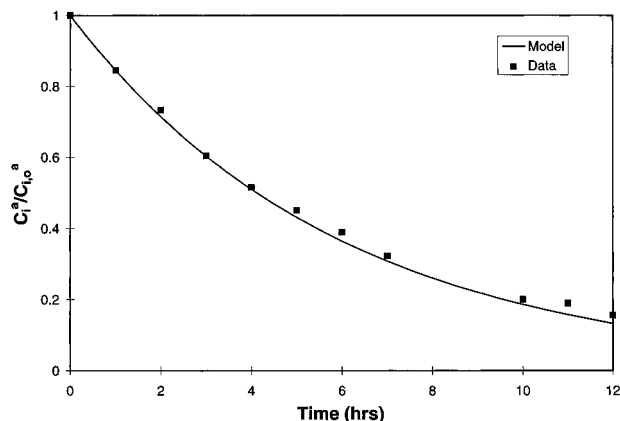


FIGURE 2. Effectiveness of aqueous phase mixing at 39 rpm normalized CaCl_2 concentration ($C_i^a/C_{i,0}^a$) profile.

The mass transfer experiments were conducted within a hood under ambient conditions with no specific provisions for temperature control, although the room temperature was recorded to be steady within the range of 20–25 °C over the course of all experiments. A Teflon-coated magnetic stir bar was placed in the bottom of the DNAPL reservoir at the outset of each mass transfer experiment. The reactor was then partially filled with water (about 200 mL) and placed on a magnetic stirrer. A 20-mL volume of DNAPL mixture was then gradually introduced through the water using a syringe fitted to a pipetting needle in a manner that ensured an undisturbed interface at the top of the cylindrical reservoir. To do this, it was essential to exclude all air droplets from the syringe prior to injection. Water was subsequently admitted through the side inlet (at a flow rate of about 5 mL/min) to the level of the overflow tube, corresponding to an overall volume of between 700 and 800 mL over a period of about 2 h. Aqueous phase stirring was initiated as soon as the impeller was completely submerged (i.e., before the aqueous phase was completely filled), and the NAPL phase stirring was also started at this time. The pump was turned off once the reactor was filled to the desired level. The aqueous phase was then sampled immediately, and this sampling time was noted as the initial time. Because the aqueous and DNAPL phases were in contact over a time period of about 2 h as the reactor was filled, the aqueous phase concentrations corresponding to the initial time were non-zero values. The aqueous phase was sampled regularly over a period of 5–7 days until equilibrium was achieved between the two phases. The DNAPL phase was sampled at the beginning and at the end of each study. All samples were diluted in methanol immediately after collection to prevent loss of component PAHs. Dilution factors used for the aqueous and DNAPL samples were 1.5–2 and 1000, respectively.

Analytical Methods. Because of large differences in the concentration ranges involved, different analytical techniques were used for analyzing the DNAPL and aqueous phase samples. Aqueous phase concentrations were analyzed using a Hewlett Packard 1090 high-performance liquid chromatograph (HPLC), equipped with a diode array detector (DAD) and a fluorescence detector (FLD). A 125 mm \times 3.2 mm reverse phase octadecylsilane column with a 5- μm packing diameter (Envirosep-PP, Phenomenex) was employed. The chromatographic conditions were programmed for an acetonitrile–water gradient elution at a constant flow rate of 0.5 mL/min and a constant temperature of 35 °C over a 35-min program run. The acetonitrile–water gradient elution consisted of 55% acetonitrile for 5 min, increasing over a linear gradient to 70% at 30 min, remaining constant at 70% up to 32 min of total elapsed time, and then falling sharply back to a constant level of 55% through the end of the run. A 15- μL volume of sample was injected. The DAD detector

signal at 220 nm and the FLD detector (time programmed with respect to gain, and emission and excitation wavelengths) were used to quantify all compounds of interest.

DNAPL phase concentrations of all components were determined using a Hewlett Packard 5890A gas chromatograph (GC) equipped with a flame ionization detector and a 5% phenyl methyl DB5 (J&W Scientific) megabore column (length 30 m, inner diameter 0.53 mm, and film thickness 1.5 μm). Oven temperature programming was set at 60 °C for 5 min, followed by a linear increase of 10 °C/min to 250 °C, at which point the temperature was held constant through the end of the 35-min run. The injector and detector temperatures were set at 250 and 300 °C, respectively. A 3- μL volume of sample was injected. Mixed PAH/methanol external standards bracketing the unknown concentrations were used for both aqueous and DNAPL phase samples; duplicate injections were made for all samples and standards.

Mass Transfer Rate Data Analysis. The batch systems tested contained DNAPL mixtures composed of hydrophobic PAH compounds at a relatively high DNAPL–water volume ratio (≥ 0.025). The total mass of PAHs transferred to the aqueous phase is small in such systems, and the DNAPL composition and aqueous phase volume can each be assumed to remain essentially constant (as suggested by preliminary mass balance calculations). Negligible changes in DNAPL constituent mole fractions over time imply constant equilibrium aqueous phase concentrations. It is to be emphasized that, while this assumption is valid in the batch systems employed here, it may be invalid in flow-through systems having large flow rates or in the presence of additional aqueous phase sinks over longer time scales, i.e., of the order of years (26, 27). Because the assumption is valid here, the aqueous phase mass balance including a source term to account for mass transfer can be expressed as follows:

$$V^a \frac{dC_i^a}{dt} = A^\circ k_{f,i} (C_{e,i}^a - C_i^a) \quad (4)$$

where A° is the interfacial area and k_f is the film mass transfer coefficient. With the initial conditions specified as, $C_i^a = C_{i,0}^a$ at $t = t_0$, eq 4 can be solved analytically to give

$$C_i^a = C_{e,i}^a - (C_{e,i}^a - C_{i,0}^a) \exp\left(-\frac{A^\circ k_{f,i} (t - t_0)}{V^a}\right) \quad (5)$$

Experimentally measured aqueous phase concentration–time profiles were fitted with this analytical expression. The initial condition was represented by the first point in time at which concentration measurements were made. Values for two fitting parameters, the aqueous phase concentration in equilibrium with the DNAPL, $C_{e,i}^a$, and the area-lumped mass transfer coefficients, $A^\circ k_{f,i}$, and, their respective 95% confidence intervals were obtained using a nonlinear parameter estimation routine (SYSTAT Inc., Evanston, IL). The parameter estimates were obtained by the method of least squares, i.e., by minimization of the sum of squared residuals achieved by the quasi-Newton method, an iterative numerical search scheme. Use of an alternate search scheme (the Simplex method) and choice of various initial guesses covering a wide range had no impact on the parameter estimates, indicating the robustness of the estimation procedure. The 95% confidence intervals on the estimates reflect their precision, which depends on the residual sum of squares, the number of concentration measurements, and the times at which measurements were made along the profile (28).

The equilibrium aqueous phase concentration values were translated to DNAPL phase activity coefficient values by rearranging eq 1, and the lumped mass transfer coefficients were converted to film mass transfer coefficients by assuming

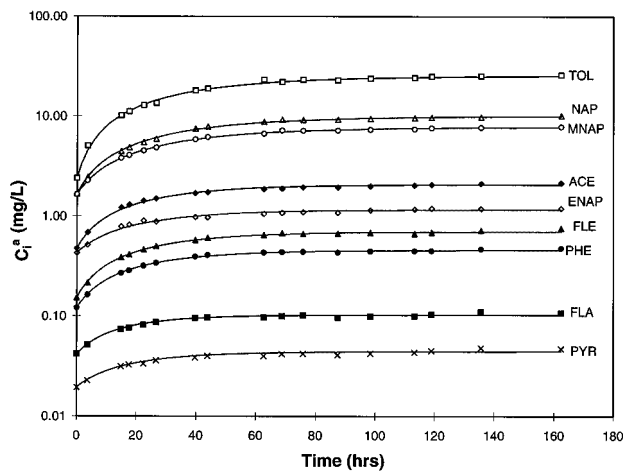


FIGURE 3. Model fit to aqueous concentration (C_a) profiles for DNAPL-III.

that the interfacial area was the same as the cross-sectional area of the reactor at the interface location, i.e., 4.9 cm².

Results and Discussion

The performance of the reactor was first evaluated by conducting two replicate runs with a single-component DNAPL, 1-methylnaphthalene. The DNAPL was stained with an organic soluble dye, Oil Red-O, to enhance the visibility of the interface. Equation 5 was found to provide a good fit to the experimental data, yielding values of 27.6 (± 0.2) and 27.8 (± 0.3) mg/L for the equilibrium aqueous phase concentration and values of 1.3×10^{-3} ($\pm 0.3 \times 10^{-4}$) and 1.4×10^{-3} ($\pm 0.6 \times 10^{-4}$) cm/s for the film transfer coefficient, $k_{f,i}$, in the two runs, respectively. The confidence interval for estimates of the film transfer coefficient does not incorporate the inherent error or variability in interfacial area between experimental runs, thus the reproducibility of this parameter reflects the relative stability of the interface. The closeness of $C_{e,i}^a$ values to the solubility limit of 28 mg/L for 1-methylnaphthalene confirms that two-parameter fits of aqueous phase profiles to eq 5 can provide reliable estimates of aqueous phase equilibrium concentration. This technique is in fact superior to the batch-equilibration technique commonly used for determining equilibrium aqueous phase concentration. The latter may lead to underestimates if insufficient time is allowed for equilibration and may lead to overestimates due to the formation of dispersions and microcrystals that cannot be easily detected or removed.

Three replicate mass transfer runs were conducted for DNAPL-I, and two replicate runs were conducted for each of the other DNAPL mixtures. Equation 5 typically provided good fits to experimentally generated aqueous phase concentration profiles for all compounds comprising the complex DNAPL mixtures. Figure 3 illustrates an example of experimental data and corresponding model fits for eq 5 from a mass transfer run on DNAPL-III. A logarithmic ordinate scale is used to allow depiction of the data and model fits for all components on the same plot. Model fits were found to be inadequate for 2-ethylnaphthalene in run 2 for DNAPL-II in which the film transfer coefficient was associated with huge error bars and for pyrene and fluoranthene in run 2 for DNAPL-I and DNAPL-II due to anomalous trends in the profile—a gradual decrease after a rapid increase instead of leveling off in DNAPL-I run 2 and a sudden increase after initially rising and leveling off in DNAPL-II run 2. Excluding these specific instances, best fit values of the mass transfer parameters for all compounds across the four DNAPL mixtures studied are summarized in Figure 4a,b. No naphthalene parameter values are given for DNAPL-I because the compound was not present in this mixture. The error bars represent 95% confidence intervals.

The DNAPL phase component activity coefficient values provide greater insight for comparisons across compounds than do values of equilibrium aqueous phase concentration. If the components of these DNAPL mixtures behaved ideally, the activity coefficient values would be unity. Hence, the equilibrium aqueous phase concentrations obtained by fitting were converted to activity coefficients using eq 1. These values are depicted in Figure 4a. The mean values are based on best fit estimates of aqueous phase equilibrium concentrations, experimentally measured mole fractions, and reported values of pure compound solubilities and fugacity ratios (Table 1). The 95% confidence intervals relate only to the estimates of equilibrium aqueous phase concentrations and do not reflect errors inherent in other parameters, i.e., DNAPL phase mole fraction estimates and reported pure compound solubilities and fugacity ratios. The standard errors associated with the DNAPL phase mole fraction determinations were typically less than 1% for most compounds other than toluene, were less than 8% for toluene, and therefore are expected to be negligible in terms of their contributions to overall error in the activity coefficient estimates. Moreover, variations in DNAPL phase mole fractions over the course of an approach to equilibrium in the batch reactor were found to be negligible for all compounds (of the same order as the standard error associated with the mole fraction estimates), thereby validating the assumption inherent in eq 5.

Figure 4a clearly depicts that not all compounds in the DNAPL mixtures studied conform to Raoult's law prediction of unit activity, even though these mixtures are comprised by structurally similar components. Toluene consistently shows a positive deviation, with activity coefficient values in the range of 1.1–1.3. 1-Methylnaphthalene and 2-ethylnaphthalene are generally in good agreement with Raoult's law, with activity coefficients ranging between 0.9 and 1.1. All other compounds manifest negative deviations, i.e., activity coefficient values less than unity. Pyrene shows the greatest deviation with activity coefficient values in the range of 0.3–0.5. This compound-specific trend in observed deviations in the DNAPL phase activity coefficient values from unity is consistent across the DNAPL mixtures.

The deviations of these activity coefficients from unity may be due either to failure of Raoult's law or to errors in input parameters (i.e., pure compound solubility or fugacity ratio estimates) that are not depicted by the error bars shown in Figure 4a. For compounds that exist as liquids at ambient temperatures, the fugacity ratio is always unity and thus does not contribute to errors in the activity coefficients. For PAHs that exist as solids at ambient temperatures, the fugacity ratio estimates derived using a constant entropy of fusion of 13.5 cal mol⁻¹ K⁻¹ for all compounds and neglecting the contribution of the specific heat terms (i.e., the values in Table 1) can potentially lead to significant errors. The experimentally measured entropy values of the PAHs of interest lie in a range of about 14–9 cal mol⁻¹ K⁻¹ (23). To determine the impact of fugacity ratio estimates on the activity coefficients, an attempt was made to refine the fugacity ratio estimates and re-determine activity coefficients. The fugacity ratio can be estimated based on thermodynamics properties (24):

$$\ln(f_i^s/f_i^l) = -\frac{\Delta H_i^f}{RT} \left(1 - \frac{T}{T_{t,i}}\right) + \frac{\Delta Q_{H,i}^0}{R} \left(\left(\frac{T_{t,i}}{T}\right) - \ln\left(\frac{T_{t,i}}{T}\right)\right) \quad (6)$$

where R is the universal gas constant; T_i is the triple point temperature in K, which is typically assumed to be same as the melting point temperature; ΔH_i^f is the enthalpy of fusion, which can be expressed as the product of triple point temperature and the entropy of fusion; and $\Delta Q_{H,i}^0$ is the difference in the constant-pressure specific heat capacity of the pure liquid and the pure solid. Refined fugacity ratio estimates were obtained using eq 6 and pure compound

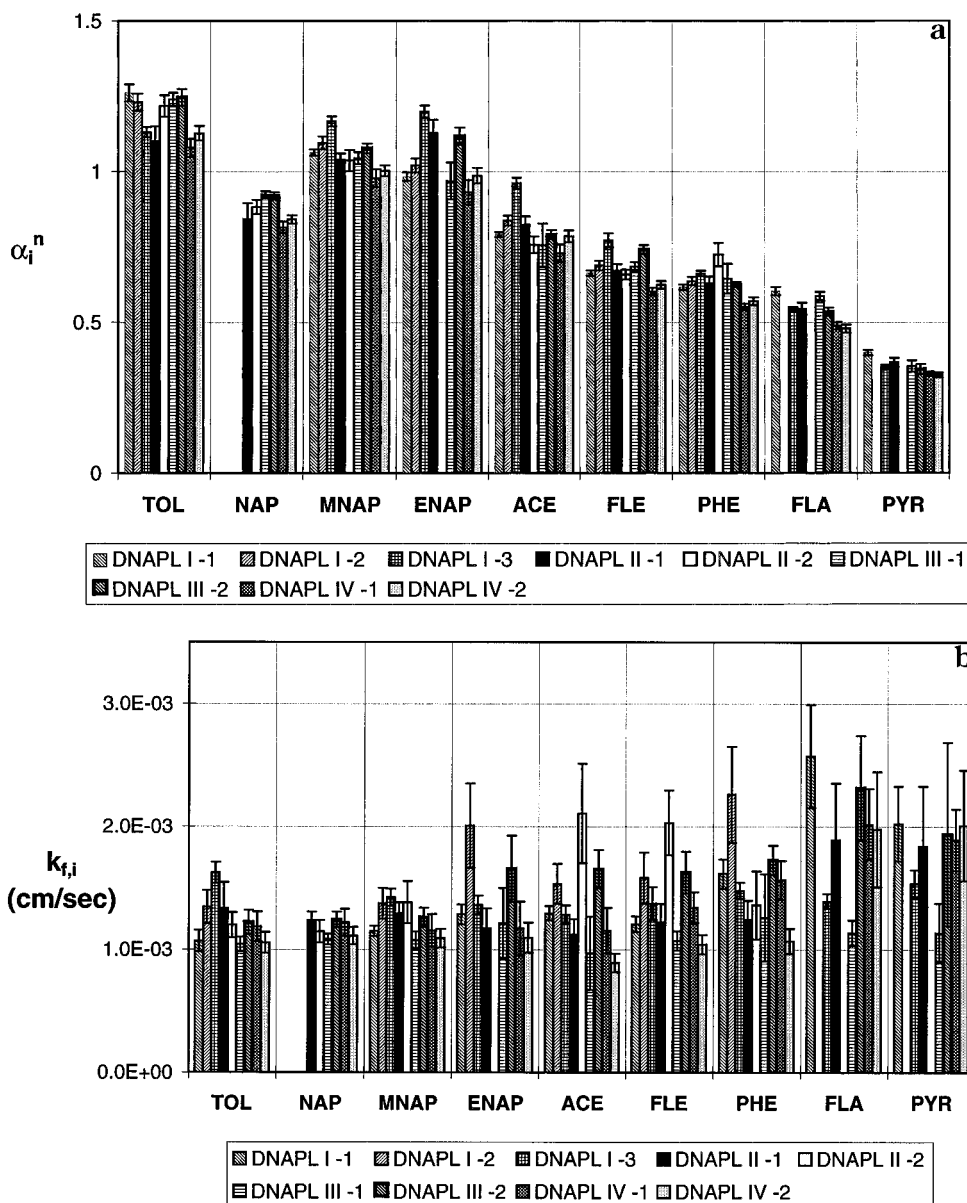


FIGURE 4. (a) Variations in DNAPL phase component activity coefficients (α_i^n). (b) Variations in component film transfer coefficients ($k_{f,i}$).

TABLE 3. Refined Fugacity Ratio Estimates for Solid Components

component	ΔH^f (cal/mol)	ΔQ_H^\ddagger (cal mol ⁻¹ K ⁻¹)	solid/liquid fugacity ratio (25 °C)
naphthalene	4540.4	2.38	0.306
acenaphthene	5134.4	1.53	0.201
fluorene	4683.7	0.15	0.160
phenanthrene	3938.5	3.82	0.279
fluoranthene	4480.9	8.00	0.213
pyrene	4153.1	-4.33	0.107

enthalpy values and correlations for specific heat capacities for pure solids and pure liquids given by Daubert and Danner (29). Values for ΔQ_H^\ddagger were evaluated at the melting point and assumed to remain constant over the temperature range $T-T_i$. The refined estimates for the solid PAHs along with their corresponding enthalpy and ΔQ_H^\ddagger values are listed in Table 3, and variations of the re-determined component activity coefficients across the four DNAPL mixtures are illustrated in Figure 5. The refined fugacity ratio estimates are higher than the estimates reported in Table 1, with that for pyrene being about double that given in Table 1. Ignoring the second

term on the right-hand side of eq 6 involving ΔQ_H^\ddagger leads to an underprediction of the fugacity ratio by less than about 5% for all compounds other than fluoranthene and pyrene, an underprediction of about 13% for fluoranthene, and an overprediction of about 20% for pyrene. The activity coefficients for solid PAHs determined using these fugacity ratio estimates tend to approach the Raoult's law prediction of unity. It may be noted that fugacity ratio estimates also have implications concerning DNAPL stability. However, because the preliminary estimates listed in Table 1 are underestimates, their refinement does not cause the mole fraction of solid components to exceed solubility in the NAPL phase.

The pure compound solubility values used in the activity coefficient computations are representative values for 25 °C. The range in literature reported values of solubility at 25 °C is considerable for some of the compounds of interest, as demonstrated by values compiled in Mackay et al. (23). Excluding outlier literature values, the positive and negative deviations from the values listed in Table 1 for the various compounds are as follows: 20% to -11% for toluene, 10% to -3% for naphthalene, 14% to -8% for 1-methylnaphthalene, 0.1% to -7% for 2-ethylnaphthalene, 12% to -36% for acenaphthene, 4% to -15% for fluorene, 7% to -10% for

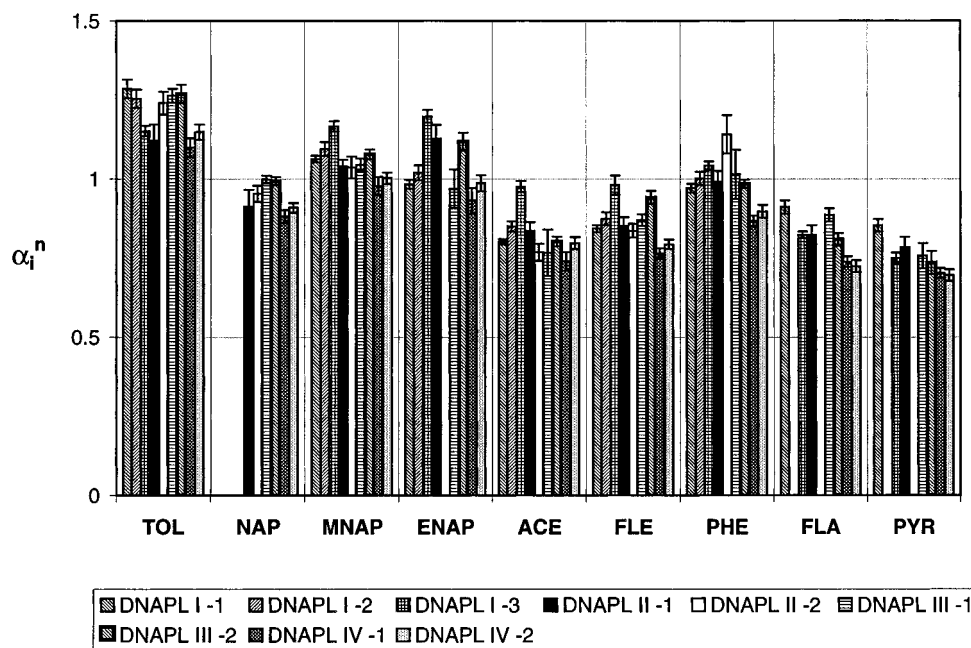


FIGURE 5. Variations in DNAPL phase component activity coefficients (α_i^n) based on refined fugacity ratio estimates.

phenanthrene, 2% to -24% for fluoranthene, and 23% to -23% for pyrene. Also, some error can be expected because there was no specific provision for temperature control in the experiments, which, as noted earlier, were conducted over a range of 20–25 °C. Based on PAH solubility values reported by Schwartz (30) at various temperatures and on solubility–temperature correlations for PAHs provided by Wauchope et al. (31) and May and Wasik (32), a decrease in temperature from 25 to 20 °C can lower the solubilities of the PAHs tested from 10 to 30%, with the higher molecular weight PAHs showing greater sensitivities to temperature fluctuations. As temperature is decreased from 25 to 20 °C, the fugacity ratio of the solid PAHs decreases by less than 15% (based on eq 6). It therefore appears that the deviations of the activity coefficients of several compounds from unity demonstrated in Figure 4a can be explained primarily by the errors associated with the preliminary fugacity ratio estimates and to some extent with errors associated with the solubility estimates and the impact of temperature fluctuations on solubility and fugacity ratios. It also appears that Raoult's law holds for these DNAPL mixtures, although its applicability may be limited by poor accuracy in input parameter values. Vadas et al. (33) reported aqueous dissolution data for PAH dissolution in benzene–water systems (with a single or multiple PAHs dissolved in benzene), which is overpredicted by the Raoult's law predictions, particularly when the subcooled liquid solubilities are derived using the preliminary fugacity ratio estimates. Lee et al. (10) implicated the error in the preliminary fugacity ratio estimate for a lack of conformity of benz[a]anthracene equilibrium concentrations to Raoult's law predictions in batch equilibration studies with coal tars. In studies with incompletely characterized environmental DNAPL mixtures, however, errors in input parameters other than fugacity ratios may play a dominant role, i.e., DNAPL phase mole fraction estimates may contain errors due to uncertainties in the bulk properties of the DNAPL phase.

Figure 4b depicts ranges of variation in estimates of the film transfer coefficients for the systems studied, assuming an interfacial area of 4.9 cm². The 95% confidence intervals in the film transfer coefficients reported are derived solely from the error in the lumped mass transfer coefficient values and do not include errors associated with the assumption of a fixed cross-sectional area as the interfacial area. This

assumption neglects interface curvature (non-zero contact angle) and oscillatory disturbance that may potentially increase the interfacial area above that of the reactor cross-sectional area. The maximum error associated with curvature of the interface (if contact angle is 90°) would reduce the film transfer coefficient values by a factor of 2. The contribution of errors due to interfacial ripples, inherent in reactors that allow direct liquid–liquid contact between adequately mixed bulk phases, were minimized by using low bulk phase stirring rates.

The mass transfer coefficients for toluene, naphthalene, and 1-methylnaphthalene are observed to fall in the range of 0.85–1.42 × 10⁻³ cm/s. Figure 4b might give an impression that the higher molecular weight PAHs have higher mass transfer coefficient values, but the wider 95% confidence intervals and significant deviations between replicate runs raise uncertainties about the actual existence of such a trend. The mass transfer coefficients for all components across all four DNAPL mixtures tested range only from 0.80 × 10⁻³ to 3.00 × 10⁻³ cm/s, and it appears reasonable to conclude that there is no statistically significant difference in the mass transfer coefficients of individual compounds with respect to each other.

Because the DNAPL mixtures studied differed primarily in their naphthalene content, it is to be expected that the film transfer coefficient for all other components will be similar across the DNAPL mixtures, as in fact is evident in Figure 4b. It is significant, however, that even the mass transfer coefficient for naphthalene remains essentially constant despite the fact that its mole fraction varied from 0.05 to 0.25. Also, the mass transfer coefficient for 1-methylnaphthalene in the single component DNAPL ($X_{1-MNap} = 1.0$) is essentially the same as in the complex DNAPL mixtures ($X_{1-MNap} = 0.29–0.22$). It can thus be concluded that there is no statistically significant trend with respect to variations in the mass transfer coefficient of a component with its DNAPL phase mole fraction, at least for the type of aromatic DNAPL mixtures considered in this study, which covered a viscosity range from 4 to 5 g cm⁻¹ s⁻¹.

With the assumption that the mass transfer resistance for hydrophobic compounds resides primarily in the aqueous-side boundary layer, the similarities in mass transfer coefficient values across the components studied can be anticipated on the basis of film diffusion theory (6); this on the

basis of the closeness of their respective free liquid diffusivity values given in Table 1 (i.e., $6.36\text{--}9.10 \times 10^{-6} \text{ cm}^2/\text{s}$). Because the diffusivities of the compounds of interest decrease by less than 15% as temperature decreases from 25 to 20 °C (determined based on the Hayduk–Laudie correlation), the lack of specific temperature control cited earlier is likely to have minimal impact on the film transfer coefficient values. Although film transfer coefficients are system specific in nature, the PAH film transfer coefficients obtained in this study ($0.80\text{--}3.00 \times 10^{-3} \text{ cm/s}$) agree well with values reported for naphthalene mass transfer from an aliphatic LNAPL film by Ghoshal et al. (17) and for phenanthrene mass transfer from various aliphatic LNAPL films by Efrogmson and Alexander (18) cited earlier in the introduction to this paper. They are also of the same order of magnitude as values reported for naphthalene mass transfer from coal tars by Ghoshal et al. (17) and for mass transfer of several aromatic compounds (e.g., toluene, naphthalene, and 1-methyl naphthalene) from LNAPL films reported by Southworth et al. (7) and Herbes et al. (19) and also cited earlier. Grimberg et al. (34) reported a film transfer coefficient of $1.67 \times 10^{-3} \text{ cm/s}$ for mass transfer of phenanthrene from a pure solid phase when the aqueous phase was stirred at 150 rpm, and Volkering et al. (35) reported values in the range of $6.6\text{--}7.7 \times 10^{-3} \text{ cm/s}$ for mass transfer from naphthalene spheres in specific size ranges with rotary shaking at 30 °C. It appears, therefore, that the values obtained in this study approach intrinsic film transfer coefficient values.

Acknowledgments

The authors would like to thank several associates at the University of Michigan, Ann Arbor: Alois M. Gerlach and Ryan O'Connor, undergraduate engineering students, for their laboratory assistance in the experimental aspects of this study; Thomas M. Young and Weilin Huang, doctoral students in the Environmental and Water Resources Engineering Program, for helpful comments; and Harald W. Eberhart, scientific master glass-blower in the College of Engineering, for fabricating the reactor. This research was funded in part by Grant ES04911 from the National Institutes of Environmental Health Superfund Program.

Abbreviations

TOL	toluene
NAP	naphthalene
MNAP	1-methylnaphthalene
ENAP	2-ethylnaphthalene
ACE	acenaphthene
FLE	fluorene
PHE	phenanthrene
FLA	fluoranthene
PYR	pyrene

Literature Cited

- (1) Neff, J. M. *Polycyclic Aromatic Hydrocarbons in the Aquatic Environment: Sources, Fates and Biological Effects*; Applied Science Publishers Ltd.: London, 1979; pp 102–115.
- (2) Enzminger, J. D.; Ahlert, R. C. *Environ. Technol. Lett.* **1987**, *8*, 269–278.
- (3) Luthy, R. G.; Dzombak, D. A.; Peters, C. A.; Roy, S. J.; Ramaswami, A.; Nakles, D.V.; Nott, B. R. *Environ. Sci. Technol.* **1994**, *28* (6), 266A–276A.
- (4) Powers, S. E.; Loureiro, C. O.; Abriola, L. M.; Weber, W. J., Jr. *Water Resour. Res.* **1991**, *27* (4), 463–477.

- (5) Miller, C. T.; Poirier-McNeill, M. M.; Mayer, A. S. *Water Resour. Res.* **1990**, *26* (11), 2783–2796.
- (6) Weber, W. J., Jr.; DiGiano, F. A. *Process Dynamics in Environmental Systems*; John Wiley and Sons: New York, 1996; Chapters 4 and 6.
- (7) Southworth, G. E.; Herbes, S. E.; Allen, C. P. *Water Res.* **1983**, *17* (11), 1647–1651.
- (8) Peters, C. A.; Luthy, R. G. *Environ. Sci. Technol.* **1993**, *27* (13), 2831–2843.
- (9) Luthy, R. G.; Ramaswami, A.; Ghoshal, S.; Merkel, W. *Environ. Sci. Technol.* **1993**, *27* (13), 2914–2918.
- (10) Lee, L. S.; Rao, P. S. C.; Okuda, I. *Environ. Sci. Technol.* **1992**, *26* (11), 2110–2115.
- (11) Lane, W. L.; Loehr, R. C. *Environ. Sci. Technol.* **1992**, *26* (5), 983–990.
- (12) Picel, K. C.; Stamoudis, V. C.; Simmons, M. *Water Res.* **1988**, *22* (9), 1189–1199.
- (13) Rostad, C. E.; Pereira, W. E.; Hult, M. F. *Chemosphere* **1985**, *14* (8), 1023–1036.
- (14) Groher, D. M. An Investigation of Factors Affecting the Concentrations of Polyaromatic Hydrocarbons in Groundwater at Coal Tar Waste Sites. Master's Thesis, Massachusetts Institute of Technology, Boston, MA, 1990.
- (15) Ahn, B. S.; Lee, W. K. *Ind. Eng. Chem. Res.* **1990**, *29*, 2927–2935.
- (16) Levins, D. M.; Glastonbury, J. R. *Trans. Inst. Chem. Eng.* **1972**, *50*, 132–146.
- (17) Ghoshal, S.; Ramaswami, A.; Luthy, R. G. *Environ. Sci. Technol.* **1996**, *30* (4), 1282–1291.
- (18) Efrogmson, R. A.; Alexander, M. *Environ. Sci. Technol.* **1994**, *28* (6), 1172–1179.
- (19) Herbes, S. E.; Southworth, G. E.; Allen, C. P. *Water Res.* **1983**, *17* (11), 1639–1646.
- (20) Nelson, E. C.; Ghoshal, S.; Edwards, J. C.; Marsh, G. X.; Luthy, R. G. *Environ. Sci. Technol.* **1996**, *30* (3), 1014–1022.
- (21) Lyman, W. J.; Reehl, W. F.; Rosenblatt, D. H. *Handbook of Chemical Property Estimation Methods*; American Chemical Society: Washington, DC, 1990; Chapter 17.
- (22) Lide, D. R.; Frederikse, H. P. R. *CRC Handbook of Chemistry and Physics*, 76th ed.; CRC Press: Boca Raton, 1996.
- (23) Mackay, D.; Shiu, W. Y.; Ma, K. C. *Illustrated Handbook of Physical–Chemical Properties and Environmental Fate for Organic Chemicals: Vol. 1 and 2*; Lewis Publishers: Chelsea, MI, 1992.
- (24) Prausnitz, J. M. *Molecular Thermodynamics of Fluid Phase Equilibria*; Prentice Hall Inc.: Englewood Cliffs, NJ, 1969; Chapter 9.
- (25) Peters, C. A.; Mukherji, S.; Knightes, C. D.; Weber, W. J., Jr. Submitted for publication in *Environ. Sci. Technol.*
- (26) Peters, C. A.; Labieniec, P. A.; Knightes, C. D. Multicomponent NAPL Composition Dynamics and Risk. In *Proceeding of ASCE National Conference on NAPLs in the Subsurface Environment: Assessment and Remediation*, Washington, DC, Nov 1996; pp 681–692.
- (27) Mackay, D.; Shiu, W. Y.; Maijanen, A.; Feenstra, S. *J. Contam. Hydrol.* **1991**, *8*, 23–42.
- (28) Berthouex, P. M.; Brown, L. C. *Statistics for Environmental Engineers*; Lewis Publishers: Chelsea, MI, 1994; Chapter 25.
- (29) Daubert, T. E.; Danner, R. P. *Physical and Thermodynamic Properties of Pure Chemicals—Data Compilations*; Hemisphere Publishing Co.: Bristol, PA, 1989.
- (30) Schwarz, F. P. *J. Chem. Eng. Data* **1977**, *22* (3), 273–277.
- (31) Wauchope, R. D.; Getzen, F. W. *J. Chem. Eng. Data* **1972**, *17* (1), 38–41.
- (32) May, W. E.; Wasik, S. P.; Freeman, D. H. *Anal. Chem.* **1978**, *50* (7), 997–1000.
- (33) Vadas, G. G.; MacIntyre, W. G.; Burris, D. R. *Environ. Toxicol. Chem.* **1991**, *10*, 633–639.
- (34) Grimberg, S. J.; Nagel, J.; Aitken, M. D. *Environ. Sci. Technol.* **1995**, *29* (6), 1480–1487.
- (35) Volkering F.; Breure, A. M.; VanAndel, J. G. *Appl. Microbiol. Biotechnol.* **1993**, *40*, 535–540.

Received for review March 12, 1996. Revised manuscript received October 8, 1996. Accepted October 8, 1996.®

ES960227N

® Abstract published in *Advance ACS Abstracts*, December 15, 1996.